JACS
JOURNAL OF THE AMERICAN CHEMICAL SOCIETY

COMMUNICATION

pubs.acs.org/JACS

Photoelectrochemical Hydrogen Evolution Using Si Microwire Arrays

Shannon W. Boettcher,[⊥] Emily L. Warren, Morgan C. Putnam, Elizabeth A. Santori, Daniel Turner-Evans, Michael D. Kelzenberg, Michael G. Walter, James R. McKone, Bruce S. Brunschwig, Harry A. Atwater,* and Nathan S. Lewis*

Kavli Nanoscience Institute and Beckman Institute, 1200 East California Boulevard, California Institute of Technology, Pasadena, California 91125, United States

Supporting Information

ABSTRACT: Arrays of B-doped p-Si microwires, diffusion-doped with P to form a radial n^+ emitter and subsequently coated with a 1.5-nm-thick discontinuous film of evaporated Pt, were used as photocathodes for H_2 evolution from water. These electrodes yielded thermodynamically based energy-conversion efficiencies >5% under 1 sun solar simulation, despite absorbing less than 50% of the above-band-gap incident photons. Analogous p-Si wire-array electrodes yielded efficiencies <0.2%, largely limited by the low photovoltage generated at the p-Si/H_2O junction.

One approach to achieving efficient solar-driven water splitting is to utilize dual light absorbers, with one absorber acting as a photocathode and the other as a photoanode.[1] Such tandem designs, in principle, allow the use of relatively small-band-gap (i.e., 1.1−1.7 eV) light absorbers that are well-matched to the solar spectrum while simultaneously providing the necessary overall photovoltage (>1.23 V) required under standard conditions to produce H_2 and O_2 from H_2O. The use of a tandem structure also relaxes the stability requirements of the light absorbers, facilitating the use of photocathodes that are stable under cathodic (but not necessarily anodic) conditions, in combination with photoanodes that are stable under anodic (but not necessarily cathodic) conditions.

Si is an attractive candidate for a tandem-system photocathode, because Si is earth-abundant, is relatively cathodically stable, has a suitable band gap, and in principle can produce a significant portion of the total photovoltage needed for water splitting. Si wire arrays have attracted attention for solar-energy-conversion applications, because the use of wire arrays allows orthogonalization of light absorption and charge-carrier collection, facilitating the use of readily grown, relatively low diffusion-length material while still offering the potential for high energy-conversion efficiencies.[2−8]

We report herein the use of p-Si and n^+p-Si wire-array photocathodes for the production of H_2 from water. The Si wires were grown by a templated vapor−liquid−solid growth process,[9] using an earth-abundant metal catalyst, Cu, and a readily available Si precursor, $SiCl_4$, in an atmospheric-pressure chemical vapor deposition system. The lithographic template used in this work produced wires that were ∼2.8 μm in diameter and were arranged on a square lattice with a center-to-center pitch of 7 μm.

Growth was performed for ∼30 min at 1000 °C to produce wires 40−60 μm in length. The wires were doped p-type during growth with BCl_3 to produce carrier concentrations of $\sim 10^{17}$ cm^{-3}, as determined by four-point probe measurements on individual wires.[5] Scanning photocurrent measurements demonstrated that these wires had minority-carrier diffusion lengths of >30 μm.[11] Some wire arrays were subsequently processed to introduce an n^+-doped emitter shell, producing a radial n^+p junction in each wire.[11,12] The performance of the wire-array electrodes was compared to that of similarly processed planar (100)-oriented single-crystalline Czochralski-grown p-Si electrodes (0.7 Ω cm resistivity).

Figure 1a,b compares the current density−potential (J−E) behavior of planar and wire-array p-Si electrodes in aqueous pH

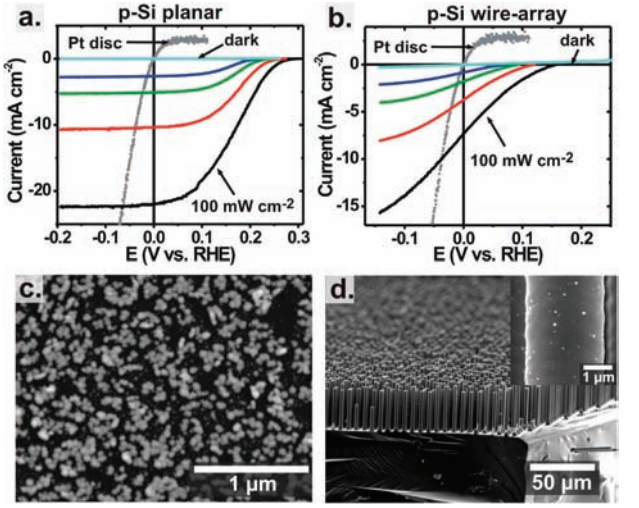

Figure 1. J−E data for (a) planar and (b) wire-array Pt/p-Si electrodes measured in aqueous 0.5 M K_2SO_4 solution adjusted to pH ∼2 with H_2SO_4 (20 mV s^{-1}, single sweep from positive to negative potentials). This pH gave the best performance, apparently due to competition between the reduced Pt activity at higher pH's and the reduced open-circuit voltages (V_{oc}) we observed at lower pH's. The solution was pre-electrolyzed between two carbon electrodes for 24 h to remove impurities.[10] The J−E data are referenced to the thermodynamic H_2 evolution potential in the solution ($E(H^+/H_2)$ = −0.362 vs SCE) and were collected at light intensities of 0, 11, 23, 48, and 100 mW cm^{-2} using ELH-type W-halogen solar simulation. The J−E data for the wire arrays were collected with the sample tilted ∼35°, to maximize the measured photocurrent (see below). The J−E behavior of a polished Pt-disk electrode is also plotted. Rapid stirring was used to minimize effects due to bubble production. SEM images of the (c) planar and (d) wire-array electrodes show the presence of Pt particles ∼20−60 nm in diameter. These specific wires were ∼40 μm long and ∼2.6 μm in diameter.[5,9]

Received: October 10, 2010
Published: January 7, 2011

Table 1. Electrode Parameters for Platinized Si Hydrogen-Evolving Photocathodes (100 mW cm^{-2} ELH illumination)

type	V_{oc} (V)	J_{sc} (mA cm^{-2})	ff	η (%)	diode quality factor, n	no. of samples
Pt/p-Si planar	0.30	23	0.3	2.1	1.3	1[a]
Pt/p-Si wires	0.16	7.3	0.18	0.21	1.6	1[a]
Pt/n$^+$p-Si planar	0.56 ± 0.01	28 ± 1	0.60 ± 0.02	9.6 ± 0.9	1.8 ± 0.1	5
Pt/n$^+$p-Si wires	0.54 ± 0.01	15 ± 2	0.71 ± 0.02	5.8 ± 0.5	1.10 ± 0.04	8

[a] The photocathode efficiency of the Pt/p-Si devices (planar and wires) was strongly dependent on the platinization procedure and also decayed with time. The reported data are the initial performance of the best p-Si samples obtained by the Pt deposition procedure outlined in the SI. The n$^+$p-Si samples, in contrast, showed stable and reproducible performance, with the average Pt/n$^+$p-Si performance far superior to the best Pt/p-Si samples.

~2 electrolyte. Prior to measurement, Pt was deposited onto the electrodes by immersion for ~10 min in an aqueous solution that contained 0.5 M HF and 1 mM K_2PtCl_6 (Figure 1c,d; see Supporting Information for details).[13] The open-circuit voltage (V_{oc}), fill factor (ff), short-circuit photocurrent density (J_{sc}), and energy conversion-efficiency (η) measured under 100 mW cm^{-2} of ELH-type W-halogen solar simulation[14] for the best planar and wire-array Pt/p-Si electrodes are listed in Table 1. The diode quality factor was extracted from the light-intensity dependence of V_{oc} (see SI).

The V_{oc} was determined relative to the reversible hydrogen electrode (RHE) potential in the electrolyte used. Research-grade H_2 was continuously bubbled through the solution to keep the Nernstian potential $E(H^+/H_2)$ constant. J_{sc} was defined as the magnitude of the photocurrent density at $E(H^+/H_2)$. The photoelectrode efficiency was calculated as

$$\eta = \frac{-i_{max}(E_{max} - E(H^+/H_2))}{P_{in}A} \quad (1)$$

where i_{max} is the current (mA) at maximum power, E_{max} is the electrode potential at maximum power (V vs SCE), $E(H^+/H_2)$ is the Nernst potential for H_2 evolution (V vs SCE) in the electrolyte, P_{in} is the incident optical power density (mW cm^{-2}), and A is the electrode area (cm^2).[15] The efficiency of the photocathode is thus referenced to a hypothetical, ideally nonpolarizable cathode that would operate with no overpotential losses at $E(H^+/H_2)$.[16] The three-electrode photoelectrochemical performance data, therefore, do not include losses that might be present at the counter electrode in a two-electrode tandem or voltage-assisted photoelectrolysis system.

A predominant factor that limited the energy-conversion efficiency of both the planar and wire-array p-Si photocathodes was the relatively low V_{oc} of the p-Si/H_2O junction. The observed V_{oc} values are consistent with prior studies of p-Si/H_2O interfaces, which indicate that the potential of the Si valence-band edge is not sufficiently positive with respect to $E(H^+/H_2)$ to produce a high photovoltage (Figure 2a).[13,17] The Pt/p-Si photocathodes also exhibited relatively low fill factors at all light intensities, consistent with the presence of a thin oxide barrier at the Pt−Si interface, formed during Pt deposition, that impeded interfacial charge transport. Likewise, $J-E$ data collected in the dark for similarly platinized p$^+$-Si electrodes showed a large series resistance compared to the Pt disk electrode. In contrast, p-Si (and p$^+$-Si) electrodes with discontinuous 1-nm-thick electron-beam-evaporated Pt films exhibited dark hydrogen-evolution activity similar to that of the polished Pt disk electrode,

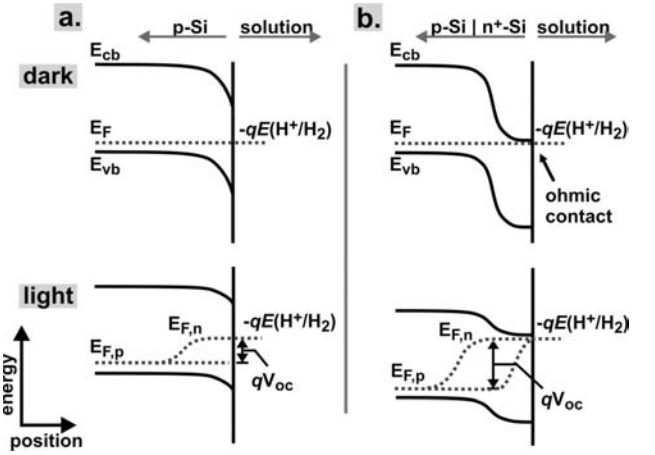

Figure 2. Band bending in (a) p-Si and (b) n$^+$p-Si photocathodes in contact with the H^+/H_2 redox couple in solution. The top diagrams show the interfaces in the dark, whereas the bottom diagrams show the interfaces under illumination. E_{cb} is the conduction band edge, E_{vb} the valence band edge, and E_F the Fermi level. $E_{F,p}$ and $E_{F,n}$ are the hole and electron quasi-Fermi levels, respectively, under illumination. The photovoltage (V_{oc}) is larger for n$^+$p-Si samples due to increased band bending at the n$^+$/p interface relative to the aqueous solution/p-Si interface.

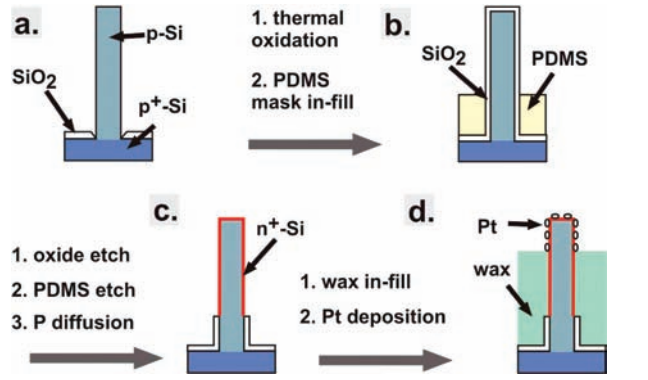

Figure 3. p-Si wire arrays with Cu growth catalyst previously removed were processed into Pt/n$^+$p-Si wire arrays following the steps outlined above. Details of the experimental procedure are in the SI.

indicating the presence of an ohmic contact between p-Si and Pt in the absence of an interfacial oxide.

To overcome these drawbacks, a buried metallurgical n$^+$p junction was introduced into the Si wires. Figure 2 shows how the buried junction decouples the band bending and photovoltage characteristics of the electrode from the energetics of the semiconductor/liquid contact.[18,19] The general scheme for the fabrication of such n$^+$p radial junctions is presented in Figure 3. For comparison, an n$^+$ emitter was also diffused into p-Si wafers to yield planar n$^+$p junctions (see SI).

To provide an electrocatalyst for H_2 evolution, Pt was deposited onto the planar and wire-array n$^+$p electrodes via electron-beam evaporation. For the planar electrodes, ~1 nm of Pt was deposited, which coalesced into sub-micrometer Pt particulate islands (Figure 4c). Evaporated Pt was used because it yielded electrodes with much higher fill factors than those subjected to electroless/electroplated Pt deposition, consistent with the $J-E$ data measured for evaporated Pt on n$^+$-Si electrodes (Figure 4a). The wire arrays were first partially filled with wax (Figure 4d inset), and a planar-equivalent thickness of 1.5 nm of

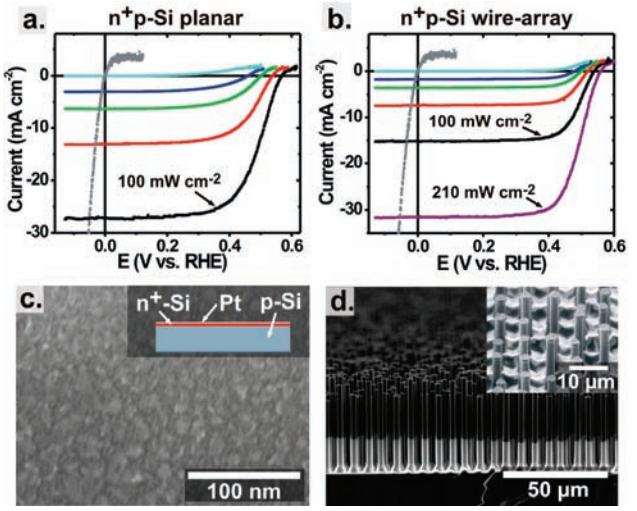

Figure 4. Pt/n^+p-Si (a) planar and (b) wire-array $J-E$ data obtained in ultrapure aqueous 0.5 M H_2SO_4. The data were collected as a single sweep from positive to negative potentials at 20 mV s^{-1} (hysteresis was not observed on the return sweep). The acidic electrolyte was used to maximize the catalytic activity of the Pt film. The $J-E$ data are referenced to the reversible hydrogen potential in the solution ($E(H^+/H_2)$ = −0.273 vs SCE) and were collected at light intensities of 0, 11, 23, 48, 100, and 210 mW cm^{-2} using ELH-type solar simulation. For reference, $J-E$ data are also plotted for a sample of n^+-Si with 1 nm of electron-beam-evaporated Pt. Rapid stirring was used to minimize effects due to the production of bubbles. The photocurrent measured for the wire-array sample was angle-dependent, with the data collected at $\theta \approx 35°$ shown here. (c) SEM image of the Pt layer deposited on the planar electrode; inset, cross-section of the electrode architecture. (d) SEM image of an n^+p-Si wire array; inset, tilted SEM image of an electrode after partial infilling with wax. The wires were typically between 40 and 60 μm in length and ∼2.4 μm in diameter (after junction fabrication).

Pt was evaporated onto the top portion of the wires. The wax infiltration prevented the evaporated Pt, which formed an ohmic contact to both the n^+ shell and the p-type wire core, from causing shunts at defective/broken wires present near the bottom of the wire array. The conductive n^+ shell transported collected electrons vertically to the catalyst-coated tips of the wires.

Figure 4 compares the $J-E$ behavior of typical planar and wire-array Pt/n^+p-Si electrodes. Average photoelectrode parameters are given in Table 1. The high V_{oc} is consistent with the presence of a buried metallurgical p−n junction with low dark/recombination current. The high fill factor is consistent with the high electrocatalytic performance of the thin Pt film in acidic aqueous electrolytes and with a low-resistance contact between the n^+-Si and the Pt. Increasing the incident light intensity such that J_{sc} > 30 mA cm^{-2} marginally decreased the ff of the wire-array electrodes to 0.68 ± 0.02, suggesting that the amount of Pt added to the exposed wire tips would be sufficient to sustain, with minimal overpotential, the current densities associated with a wire-array device that absorbed all of the incoming light at 1 sun Air Mass 1.5 illumination conditions.

Integrating-sphere optical measurements have revealed that the optical absorption is minimized when Si wire arrays are oriented at normal incidence relative to a direct-beam illumination source.[20] As shown in Figure 5a, the short-circuit photocurrent density of the Pt/n^+p-Si wire arrays increased when the electrode was tilted relative to the incident beam direction until $\theta \approx 35°$, at which point the improved absorption was offset by the

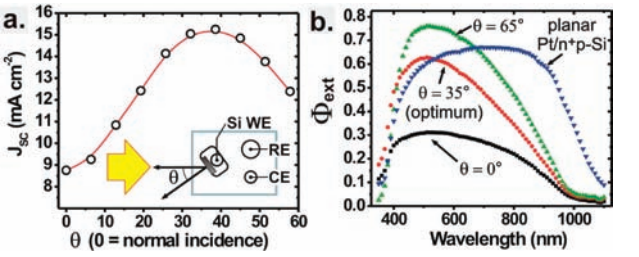

Figure 5. (a) Angular dependence of the short-circuit photocurrent density for a Pt/n^+p-Si wire-array sample measured under 100 mW cm^{-2} of ELH illumination. The beam size was much larger than the sample area. (b) Spectral response of the Pt/n^+p-Si planar and wire-array samples that displayed the $J-E$ behavior shown in Figure 4. For spectral response measurements, the beam spot was smaller than the sample area so that, for each angle, the entire beam remained on the sample. Although Φ_{ext} was higher for all wavelengths at $\theta = 65°$ than at $\theta = 35°$, the observed photocurrent decreased for $\theta > 35°$, because the absolute number of photons incident onto the surface is proportional to cos(θ).

decreased photon flux that struck the electrode at higher angles of incidence.

Figure 5b shows the typical spectral response for the planar and wire-array Pt/n^+p-Si electrodes. The planar electrode showed a peak external quantum yield, Φ_{ext}, of ∼0.65, consistent with reflection losses at the Si−water interface and weak absorption by the thin Pt film. The large decrease in Φ_{ext} for λ < 400 nm can be attributed to poor charge-carrier collection in the n^+ emitter, which could be improved by optimization of the doping parameters.[21] The spectral response for the wire-array electrode, with Φ_{ext} peaking near 500 nm, is consistent with the published optical absorption of the wire arrays.[20] When the wire arrays were tilted relative to the incident beam, the peak Φ_{ext} value increased to 0.76, demonstrating that the internal quantum efficiency (Φ_{int}) for charge collection in this radial Pt/n^+p-Si architecture is ≥0.76. Convolution of the spectral response in Figure 5b with the American Society for Testing and Materials Air Mass 1.5 global spectrum (ASTM AM1.5G) predicts a J_{sc} at $\theta = 35°$ of 13.4 mA cm^{-2}. The photocurrents measured under ELH illumination were typically ∼15% larger than the photocurrent predicted from the ASTM AM1.5G spectrum. This difference is due to the mismatch between the ASTM AM1.5G and ELH-lamp spectra and is amplified by the peaked shape of the wire-array spectral response compared with that of planar Si electrodes (Figure 5b).[14,22] Subsequent measurement of the wire-array electrodes under 100 mW cm^{-2} of Oriel Xe solar simulation with an AM1.5G filter set (which has a somewhat better match to the ASTM AM1.5G spectra, see SI) yielded J_{sc} = 13 ± 1 mA cm^{-2}, and therefore produced photoelectrode efficiencies of ∼5%.

The H_2-evolving Pt/n^+p-Si wire-array electrodes were relatively stable under cathodic conditions. After >22 h of continuous operation under 1 sun illumination, with the electrode poised potentiostatically near the maximum power point (0.4 V vs RHE), the ff of a Pt/n^+p-Si wire array electrode decreased slightly, from 0.67 to 0.62. Etching the electrode for 5 s in 10% aqueous HF restored the ff to 0.65, indicating the possible formation of a thin surface oxide due to incomplete cathodic protection. Additional efforts to protect the Si surface from oxidation should improve the durability of this system, as has been shown for Si microsphere photocathodes producing H_2 in aqueous HBr.[23]

The data presented herein demonstrate that high photovoltages, fill factors, and Φ_{int} values are achievable through the use

of radial-junction photocathodes fabricated from Si grown via a vapor−liquid−solid mechanism. The thermodynamic efficiencies of the Pt/n^+p-Si wire-array photocathodes reported here of 5−6% are higher than those measured for thin-film $CuGaSe_2$ (<1%, due to low photovoltages),[24] p-Si wafer photocathodes (2−3%) studied herein and previously,[13,17] and platinized p-WSe_2 single crystals (6−7%, but only for low-level monochromatic illumination).[25] However, the Si wire-array performance is below that reported for Rh-modified single-crystal InP (∼13%)[26,27] as well as for planar Pt/n^+p-Si samples studied herein and previously (∼10%).[18] These planar Si electrodes could themselves be substantially improved through optimization of doping, antireflective surface texture, and catalyst placement. The wire arrays, however, provide several potential advantages. They allow the use of lower-purity Si with shorter minority-carrier diffusion lengths,[4] in conjunction with the ability to transfer the partially embedded wire arrays into a flexible polymer-based electrode form factor.[28] Compared to a planar device, the wire arrays also afford an increased surface area for electrocatalyst attachment, which may be important when utilizing non-precious metal electrocatalysts with lower per-atom activities.[29]

By increasing the light absorption in the Si wire-array electrodes, it should be possible to double the energy-conversion efficiencies to values that approach those achieved for optimized single-crystal photocathodes (i.e., >10%). Structures that incorporate optical light-trapping features, including an Ag back reflector and Al_2O_3 scattering particles, have been shown to increase the absorption in Si wire arrays.[20] Preliminary measurements on electrodes with these features added yielded J_{sc} = 24.5 mA cm^{-2} under ELH-type solar simulation (see SI). However, the processing steps associated with the introduction of the light-trapping features degraded the ff (0.55) and V_{oc} (0.49 V), so the efficiency improved only marginally (η = 6.6%).

Efforts are underway to enhance light absorption while maintaining and/or improving the demonstrated photocathode properties, to replace Pt with non-precious-metal hydrogen-evolution catalysts, and to integrate these Si wire-array photocathodes with efficient photoanodes such that the direct, efficient photoelectrolysis of water, without wires or external biasing, can be achieved.

■ ASSOCIATED CONTENT

Supporting Information. Detailed procedures for growth, processing, and testing of the planar and wire-array Si electrodes; analysis of the wire-array electrodes with light trapping features; spectral irradiance curves for the light sources used. This material is available free of charge via the Internet at http://pubs.acs.org.

■ AUTHOR INFORMATION

Corresponding Author

haa@caltech.edu; nslewis@caltech.edu

Present Addresses

[⊥]Department of Chemistry, University of Oregon.

■ ACKNOWLEDGMENT

The Department of Energy (DE-FG02-05ER15754), the Stanford Global Climate and Energy Project, and Toyota are acknowledged for financial support. S.W.B thanks the Kavli Nanoscience Institute for a postdoctoral fellowship. M.G.W acknowledges support from an NSF American Competitiveness in Chemistry postdoctoral fellowship (CHE-0937048).

■ REFERENCES

(1) Bolton, J. R.; Strickler, S. J.; Connolly, J. S. *Nature* **1985,** *316*, 495.
(2) Goodey, A. P.; Eichfeld, S. M.; Lew, K. K.; Redwing, J. M.; Mallouk, T. E. *J. Am. Chem. Soc.* **2007,** *129*, 12344.
(3) Garnett, E. C.; Yang, P. D. *J. Am. Chem. Soc.* **2008,** *130*, 9224.
(4) Kayes, B. M.; Atwater, H. A.; Lewis, N. S. *J. Appl. Phys.* **2005,** *97*, 114302.
(5) Boettcher, S. W.; Spurgeon, J. M.; Putnam, M. C.; Warren, E. L.; Turner-Evans, D. B.; Kelzenberg, M. D.; Maiolo, J. R.; Atwater, H. A.; Lewis, N. S. *Science* **2010,** *327*, 185.
(6) Tian, B.; Kempa, T. J.; Lieber, C. M. *Chem. Soc. Rev.* **2009,** *38*, 16.
(7) Putnam, M. C.; Turner-Evans, D. B.; Kelzenberg, M. D.; Boettcher, S. W.; Lewis, N. S.; Atwater, H. A. *Appl. Phys. Lett.* **2009,** *95*, 163116.
(8) Yoon, H. P.; Yuwen, Y. A.; Kendrick, C. E.; Barber, G. D.; Podraza, N. J.; Redwing, J. M.; Mallouk, T. E.; Wronski, C. R.; Mayer, T. S. *Appl. Phys. Lett.* **2010,** *96*, 213503.
(9) Kayes, B. M.; Filler, M. A.; Putnam, M. C.; Kelzenberg, M. D.; Lewis, N. S.; Atwater, H. A. *Appl. Phys. Lett.* **2007,** *91*, 103110.
(10) Azzam, A. M.; Bockris, J. O. M.; Conway, B. E.; Rosenbergy, H. *Trans. Faraday Soc.* **1950,** *46*, 918.
(11) Kelzenberg, M. D.; Turner-Evans, D. B.; Putnam, M. C.; Boettcher, S. W.; Briggs, R. M.; Baek, J. Y.; Lewis, N. S.; Atwater, H. A. *Energy Environ. Sci.* **2010**, in press.
(12) Putnam, M. C.; Boettcher, S. W.; Kelzenberg, M. D.; Turner-Evans, D. B.; Spurgeon, J. M.; Warren, E. L.; Briggs, R. M.; Lewis, N. S.; Atwater, H. A. *Energy Environ. Sci.* **2010,** *3*, 1037.
(13) Lombardi, I.; Marchionna, S.; Zangari, G.; Pizzini, S. *Langmuir* **2007,** *23*, 12413.
(14) Seaman, C. H.; Anspaugh, B. E.; Downing, R. G.; Esrey, R. S. *14th IEEE Photovoltaic Spec. Conf.* **1980,** *14*, 494.
(15) Parkinson, B. *Acc. Chem. Res.* **1984,** *17*, 431.
(16) Such an ideal electrode, of course, does not exist. This method of calculating electrode efficiency thus includes losses associated with both concentration and kinetic overpotentials, as well as series resistance, and hence underestimates the actual photoelectrode performance relative to a real dark cathode for H_2 production in this same electrolyte.
(17) Dominey, R. N.; Lewis, N. S.; Bruce, J. A.; Bookbinder, D. C.; Wrighton, M. S. *J. Am. Chem. Soc.* **1982,** *104*, 467.
(18) Nakato, Y.; Egi, Y.; Hiramoto, M.; Tsubomura, H. *J. Phys. Chem.* **1984,** *88*, 4218.
(19) Nakato, Y.; Iwakabe, Y.; Hiramoto, M.; Tsubomura, H. *J. Electrochem. Soc.* **1986,** *133*, 900.
(20) Kelzenberg, M. D.; Boettcher, S. W.; Petykiewicz, J. A.; Turner-Evans, D. B.; Putnam, M. C.; Warren, E. L.; Spurgeon, J. M.; Briggs, R. M.; Lewis, N. S.; Atwater, H. A. *Nat. Mater.* **2010,** *9*, 239.
(21) Fahrenbruch, A. L.; Bube, R. H. *Fundamentals of Solar Cells*; Academic Press: San Diego, CA, 1983; p 272.
(22) Casagrande, L. G.; Tufts, B. J.; Lewis, N. S. *J. Phys. Chem.* **1991,** *95*, 1373.
(23) Kilby, J. S.; Lanthrop, J. W.; Porter, W. A. U.S. Patent 4021323, 1977; U.S. Patent 4100051, 1978; U.S. Patent 4136436, 1979.
(24) Marsen, B.; Cole, B.; Miller, E. L. *Sol. Energy Mater. Sol. Cells* **2008,** *92*, 1054.
(25) Baglio, J. A.; Calabrese, G. S.; Harrison, D. J.; Kamieniecki, E.; Ricco, A. J.; Wrighton, M. S.; Zoski, G. D. *J. Am. Chem. Soc.* **1983,** *105*, 2246.
(26) Aharon-Shalom, E.; Heller, A. *J. Electrochem. Soc.* **1982,** *129*, 2865.
(27) Heller, A. *Science* **1984,** *223*, 1141.
(28) Spurgeon, J. M.; Boettcher, S. W.; Kelzenberg, M. D.; Brunschwig, B. S.; Atwater, H. A.; Lewis, N. S. *Adv. Mater.* **2010,** *22*, 3277.
(29) Trasatti, S. *J. Electroanal. Chem.* **1972,** *39*, 163.